

# Peculiarities of the Leidenfrost effect application for drag force reduction

Jonas Gylys\*, Raminta Skvorčinskienė\*\*, Linas Paukštaitis\*\*\*

\*Kaunas University of Technology, K. Donelaičio 20, 44239 Kaunas, Lithuania, E-mail: jonas.gylys@ktu.lt

\*\*Kaunas University of Technology, K. Donelaičio 20, 44239 Kaunas, Lithuania, E-mail: raminta.skvorcinskiene@gmail.com

\*\*\*Kaunas University of Technology, K. Donelaičio 20, 44239 Kaunas, Lithuania, E-mail: linas.paukstaitis@ktu.lt

**crossref** <http://dx.doi.org/10.5755/j01.mech.20.3.6775>

## 1. Introduction

A movement of body in the fluid is affected by a drag force which resists and slows the motion. In general this resistance depends on the body's (or liquid flow) velocity, body's shape and on the physical characteristics of the liquid. Usually a drag force is characterized by the drag coefficient  $C_D$ , which is influenced by the velocity (Reynolds number) and for the spherical body are investigated quite well [1]. In order to overcome drag force and to maintain body's motion it is required a sufficient amount of energy. Therefore drag force reduction is one of the most important hydrodynamic tasks. Nowadays are known a lot of different methods allowing drag force reduction and energy economy as well. In some cases methods are used that enables density or viscosity reduction of the liquid, in other cases – methods allowing alteration of the body's surface properties. Up to today various techniques have been proposed: polymer injection or air lubrication, wall oscillation or elastic (hydrophobic and compliant) coating and etc. Main features of some of the mentioned methods are as follows:

- The polymer fluid is inserted into the boundary layer between the liquid and the body (vessel) [2]. Such polymer initially must be "preconditioned" in order to elongate its molecules. This technique enables quell turbulence and reduce skin friction immediately upon injection.

- Various air lubrication techniques are applied in order to reduce drag force [3]:

- bubble drag reduction (BDR) - small bubbles are injected into the boundary layer;
- air layer drag reduction (ALDR) - gas creates a lubricating layer between hull and liquid;
- partial cavity drag reduction (PCDR) - gas creates a lubricating layer between the part of the hull and liquid.

- Method, which was proposed by A. Vand [4] in 1945, is based on the possibility to reduce drag force by vibration of the body. As a result of that a speed of body (boat) can be higher or the same speed can be kept using less power.

- Drag reduction through elastic coating [5] with both flow and material properties considered.

One of the newest methods which help to reduce the drag force and to increase velocity of body without increasing energy consumption is so called supercavitation [6]. Supercavitation effect is based on the use of cavitation to create a large bubble of gas inside a liquid, allowing an object to move at great velocity through the liquid by being wholly enveloped by the bubble. The cavity (bubble) reduces the drag on the object, since drag is normally about

1000 times greater in liquid (water) than in a gas (air). Cavitation happens when water pressure is lowered below its vapor pressure or vapor pressure is increased to water pressure. Usually this happens at the extremely high speed although often it can happen at any speed [6]. The one of the possible modification of this method is to generate supercavitation by injecting a hot gas in front of the moving object [6]. The hot gas will vaporize water and will reduce the friction of the body to a mixture of gas and vaporized water.

Authors [7] proposed to reduce the drag force by using boiling crisis or Leidenfrost effect. In 1756 year J. G. Leidenfrost [8] observed that water droplets supported by the vapor film evaporate much slower. The Leidenfrost effect is a phenomenon in which a liquid, in near contact with a body significantly hotter than the liquid's boiling point, produces an insulating vapor layer keeping that liquid separately from the body's surface [7]. The experiments [7], which were performed by dropping spherical body into the liquid (electrolyte FC-72), showed that the spherical hot body (wrapped by the vapor film) moves 2.5 times faster than the cold body. Authors chose the electrolyte FC-72 thanks to its specific thermodynamic features: electrolyte boiling temperature at the atmospheric pressure is 56°C; density is 1680 kg/m<sup>3</sup> at the temperature 38°C and heat capacity is 1.1 kJ/kg K at the same (38°C) temperature.

Due to the fact that the analogical parameters of the other liquids, for example, water, are sufficiently different from those, mentioned above, it is reasonable to estimate the hydro and thermodynamic limits showing the acceptability of the body's heating in order to reduce drag force (or increase body's velocity).

Main task of this work is to analytically determine thermal and hydrodynamic conditions under which a boiling crisis (Leidenfrost effect) is reasonable to use for the drag force reduction of the spherical body moving in the water and electrolyte FC-72. For the main analytical analysis the body was considered that is made from the stainless steel, diameter was 0.02 m. Body's velocity was changed from 0.03 to 32.5 m/s; liquid and cold body temperature was kept at 20°C; hot body temperature was equal to 500°C.

## 2. Analytical analysis of drag force

Let assume a spherical body, which falls in the liquid vertically. In general a body can be affected by the following main forces: gravity, fluid resistance, and buoyancy (Archimedes force). If the force of gravity is greater than the Archimedes force, body moves vertically down-

wards, and otherwise - upwards. Initially body moves with acceleration. When a gravity force becomes equal to the sum of the friction (resistance) force and the buoyancy (Archimedes force), the body begins to move at a constant velocity (gradually).

Spherical cold body stabilized falling velocity can be expressed by the Eq.(1) [9], m/s:

$$w_1 = \frac{d^2(\rho_{sphere} - \rho_L)g}{18\mu_L}, \quad (1)$$

where  $d$  is body's diameter (0.02 m);  $\rho_L$ ,  $\rho_{sphere}$  are water and spherical body densities at the temperature 20°C (999.7 and 7800 kg/m<sup>3</sup> respectively);  $\mu_L$  is coefficient of the dynamic viscosity (1.308 Pa·s).

Drag force of the spherical body can be calculated using the Eq. (2) [10], N:

$$F_D = C_D \pi R^2 \frac{\rho_L w_1^2}{2}, \quad (2)$$

where  $C_D$  is drag coefficient of the spherical body (Fig. 1);  $R$  is body's radius (0.02 m);  $w_1$  is stabilized velocity of the body's fall, m/s.

Cold body drag coefficient [1] for the region  $500 \leq Re \leq 200000$  (velocity  $w \sim 0.03 \div 13.06$  m/s) is almost constant  $C_D = 0.46$ . Thus, the drag force of the cold spherical body falling in the liquid, according to the Eq. (2), is equal to 0.0474 N, where  $w_1$  is equal to 0.81 m/s (Eq. (1)).

As it was mentioned before, authors [7] (Fig. 1) determined that the stabilized falling velocity of the body, wrapped by vapor film, in comparison with velocity of the cold body, increases by 2.5 times in the electrolyte FC-72.

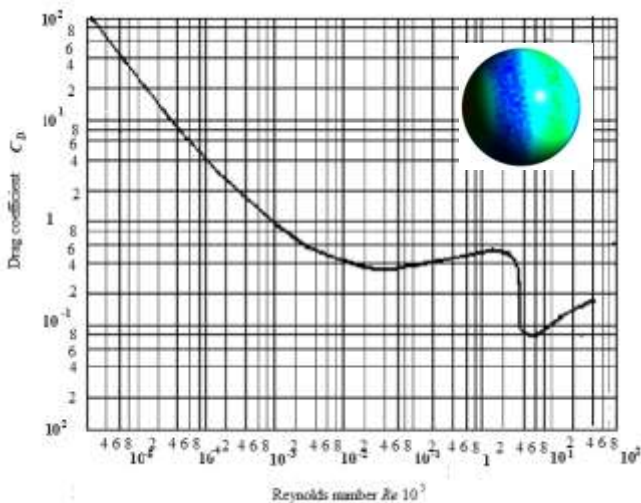


Fig. 1 Drag coefficient dependence on the Reynolds number [1]

Let's consider that the stabilized velocity of the hot spherical body falling in the water increases by the same ratio, i.e. 2.5 times. In such a case falling velocity of the hot body in water will be  $w_2 = 2.5 \cdot 0.81 = 2.03$  m/s.

It is assumed, that a vapor film enables increase falling velocity by 2.5 times if the drag force is the same as for the cold body case:  $F_D^{cold1} = F_D^{hot} = 0.0474$  N

The hot body's drag force coefficient  $C_D^{hot} = 0.074$  can be obtained from the Eq. (2):

$$C_D^{hot} = \frac{2F_D^{hot}}{\pi R^2 \rho_L w_2^2}. \quad (3)$$

At the same time drag force of the cold body, moving at the velocity  $w_2 = 2.03$  m/s, will be 0.296 N (according to the Eq. (2)).

Table shows drag force calculation options and results for the different velocities of the spherical body which  $d = 0.02$  m.

Table

Drag force of hot and cold spherical body

No.	$w_1$ , m/s	$w_2$ , m/s	$F_D^{cold1}$ , N	$F_D^{cold2}$ , N	$F_D^{hot}$ , N
1	0.81	2.03	0.047	0.296	0.047
2	1.62	4.05	0.189	1.184	0.189
3	2.43	6.08	0.426	2.665	0.426
4	3.24	8.10	0.758	4.737	0.758
5	4.05	10.13	1.184	7.401	1.184
6	4.86	12.15	1.705	10.658	1.705

## 2. Energy consumption of hot and cold bodies

The minimal value of the heat flux, necessary for the formation of a stable vapor film on the surface of the spherical body placed in the large volume of the water, can be estimated using N. Zuber equation [11, 12]:

$$q_2 = q_{min}'' = 0.09 \rho_V i_{fg} \left[ \frac{\sigma g (\rho_L - \rho_V)}{(\rho_L + \rho_V)^2} \right]^{1/4}, \quad (4)$$

where  $\rho_V$ ,  $\rho_L$  are vapor and liquid density at the boiling temperature (0.595 and 958 kg/m<sup>3</sup> respectively);  $\sigma$  is surface tension coefficient (0.0589 N/m);  $g$  is acceleration of gravity (9.81 m/s<sup>2</sup>);  $i_{fg}$  is evaporation heat (2260 kJ/kg).

Calculations according to the Eq. (4) give a value equal to  $19 \cdot 10^3$  W/m<sup>2</sup>. Taking into account a small reserve let's assume, that the heat flow, necessary for reaching boiling crisis and forming a stable vapor film is equal to  $q^{sphere} = 20 \cdot 10^3$  W/m<sup>2</sup>.

Drag force of the hot body, moving at the velocity  $w_2$  (2.5 times faster than a cold body), will remain the same as that for the cold body, moving at the velocity  $w_1$  (0.81 m/s) only in the case if the drag coefficient  $C_D$  will be equal to 0.074 (instead of 0.46). Distance, which the body moving at the same velocity ( $w_2 = 2.03$  m/s) passes during one second ( $t = 1$  s) is equal to  $L = 2.03$  m. In that case energy consumption, necessary for the hot body to overcome distance  $L$ , will be 0.096 J (according to the Eq (5)):

$$Q_1 = F_D^{hot} L. \quad (5)$$

Besides that it is necessary to evaluate an amount of energy (26.000 J) spent for the heating of the body which can be obtained from the equation:

$$Q_2 = q^{sphere} A t, \quad (6)$$

where  $A$  is area of the spherical body's surface ( $A = 4\pi r^2$ ),  $m^2$ ;  $r = d/2 = 0.01$  m;  $t = 1$  s.

Total energy consumption (26.096 J) for the hot body is calculated as follows:

$$Q^{hot} = Q_1 + Q_2 \quad (7)$$

Cold body moves at an increased velocity  $w_2 = 2.03$  m/s; the drag force is  $F_D^{cold2} = 0.296$  N. Energy consumption (0.601 J) of the cold body moving at the same velocity as the hot body ( $t = 1$  s,  $L = 2.03$  m) is obtained from:

$$Q^{cold2} = F_D^{cold2} L. \quad (8)$$

The difference of the energy consumption (25.5 J) for the hot and cold bodies', moving at the same velocity 2.03 m/s, is obtained from the equation:

$$\Delta Q = Q^{hot} - Q^{cold2}. \quad (9)$$

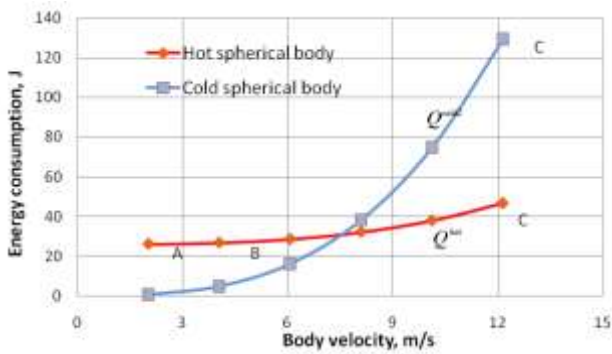


Fig. 2 Energy consumption dependence on the spherical body velocity ( $w_{hot}/w_{cold} = 2.5$ )

Energy consumption change, depending on the body's velocity, is calculated according to the Eqs. (1) to (8).

Fig. 2 shows the hot and cold bodies' energy consumption dependence on the velocity. This graph is drawn assuming, that the velocity of the hot body has no influence on a stability of the vapor film.

Fig. 2 shows that the increase of the cold or hot body's velocity influences on the energy consumption grow. For the case, if the body's velocity is greater than 7.5 m/s, the total energy consumption, required for the hot body movement, is less than that for the cold body at the same velocity. The hot body (wrapped with a vapor film) achieves the same velocity using less energy than the cold body. Otherwise the hot body moves faster using the same energy amount like the cold body. Higher velocity corresponds to the higher energy savings.

### 3. Energy relative consumption of the hot and cold bodies, moving in the water

Comparison of the energy relative consumption of the hot and cold body's, allows us better present the pro-

cess mechanism and examines the limits where the Leidenfrost effect can be used as a measure for drag force reduction.

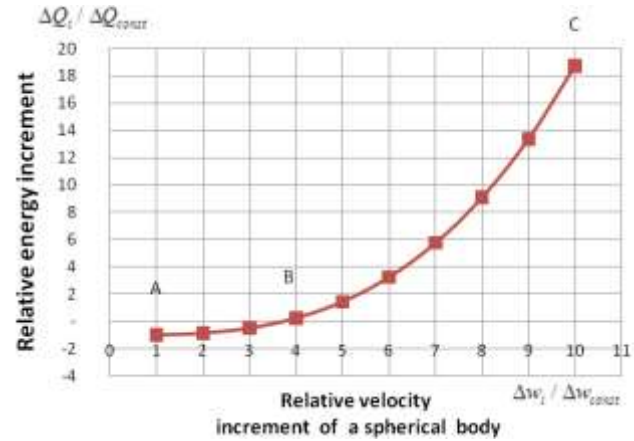


Fig. 3 Energy relative increment dependence on the body's velocity relative increment (starting point - initial stabilized velocity ( $w_2 = 2.03$  m/s))

Fig. 3 shows the influence of the velocity relative increment  $\Delta w_i / \Delta w_{const}$  on the energy relative increment  $\Delta Q_i / \Delta Q_{const}$ . Here an initial stabilized velocity of the hot body ( $w_2 = 2.03$  m/s) is taken as a starting point. In Fig. 3 segment AB, which is below zero axes, shows an area, where the energy relative consumption of the cold body is lower than that of the hot body. The curve segment BC, which is above zero axes, shows an area, where the energy relative consumption of the hot body is lower than that of the cold body.

Energy relative increment  $\Delta Q_i / \Delta Q_{const}$  is calculated as a ratio of the cold and hot bodies energy consumption difference at the  $i^{th}$  point ratio to the initial ( $i = 1$  point) energy consumption difference, where the velocity of the hot body is considered as a stabilized ( $w_2 = 2.03$  m/s) velocity.

Energy consumption difference  $\Delta Q_i$  (at the  $i^{th}$  point) is equal to, J:

$$\Delta Q_i = Q_i^{hot} - Q_i^{cold2}, \quad (10)$$

where  $Q_i^{hot}$  is hot body energy consumption at the initial ( $i = 1$ ) point, J;  $Q_i^{cold2}$  is cold body, moving at the same velocity as a hot body, energy consumption at the initial point ( $i = 1$ ), J.

Energy consumption difference  $\Delta Q_{const}$  for the velocity  $w_2 = 2.03$  m/s can be found from the equation, J:

$$\Delta Q_{const} = Q_{const}^{hot} - Q_{const}^{cold2}, \quad (11)$$

where  $Q_{const}^{hot}$  is energy consumption of the hot body at the velocity  $w_2 = 2.03$  m/s, J;  $Q_{const}^{cold2}$  is energy consumption of the cold body, moving at the same velocity as a hot body ( $w_2 = 2.03$  m/s), J.

Velocity relative increment  $\Delta w_i / \Delta w_{const}$  is the cold and hot bodies velocity difference at the  $i^{th}$  point ratio to the initial ( $i = 1$ ) point velocity difference, where the

velocity of the hot body is considered as a stabilized ( $w_2 = 2.03$  m/s) velocity.

Cold and hot bodies' velocity difference  $\Delta w_i$  at the  $i^{th}$  point, is found from the equation, m/s:

$$\Delta w_i = w_{2i} - w_{1i}, \quad (12)$$

where  $w_{2i}$ ,  $w_{1i}$  are velocity of the hot and the cold bodies at the  $i^{th}$  point, m/s.

Velocity relative increment  $\Delta w_i / \Delta w_{const}$  is the cold and hot bodies velocity difference at the  $i^{th}$  point ratio to the initial ( $i = 1$ ) point velocity difference, where the velocity of the hot body is considered as a stabilized ( $w_2 = 2.03$  m/s) velocity.

Cold and hot bodies' velocity difference  $\Delta w_{const}$  at the initial ( $i = 1$ ) point is found from the equation, m/s:

$$\Delta w_{const} = w_{2const} - w_{1const}, \quad (13)$$

where  $w_{2const}$  is stabilized velocity of the hot body ( $w_2 = 2.03$  m/s);  $w_{1const}$  is stabilized velocity of the cold body ( $w_1 = 0.81$  m/s).

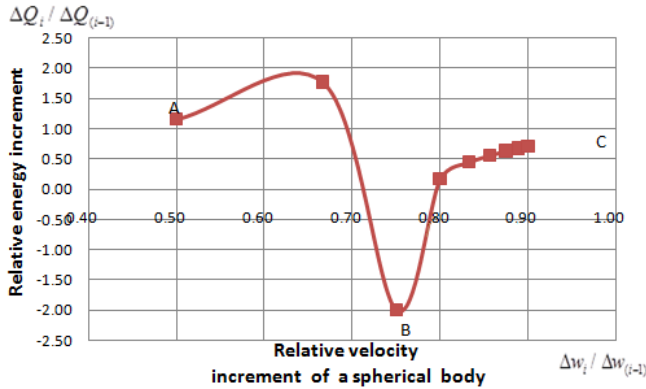


Fig. 4 Energy relative increment dependence on the body's velocity relative increment (starting point – body's preceding velocity)

Fig. 4 shows the velocity relative increment  $\Delta w_i / \Delta w_{i-1}$  influence on the energy relative increment  $\Delta Q_i / \Delta Q_{i-1}$ . Here a preceding (previous) velocity is assumed as an initial starting point. Point B can be considered as a critical point, which separates an area, where energy consumption of the hot body is higher than that of the cold body, from the area, where the energy consumption of the hot body is less than that of the cold body.

The Point B, which is below zero axes, shows an area, where the energy relative consumption of the cold body is lower than that of the hot body.

Energy consumption difference  $\Delta Q_i$  at the  $i^{th}$  point for the various velocities can be found from the Eq. (9). Energy consumption difference  $\Delta Q_{i-1}$  at the initial point is found from the equation:

$$\Delta Q_{i-1} = Q_{i-1}^{hot} - Q_{i-1}^{cold2}, \quad (14)$$

where  $Q_{i-1}^{hot}$  is hot spherical body energy consumption at the initial point ( $i = 1$ ), J;  $Q_{i-1}^{cold2}$  is cold spherical body energy consumption at the initial point ( $i = 1$ ), J.

Relative increment of the velocity  $\Delta w_i / \Delta w_{i-1}$  is the ratio of the hot and cold bodies' velocity difference at the  $i^{th}$  point to the difference at the initial ( $i = 1$ ) point.

Velocity difference  $\Delta w_i$  at the  $i^{th}$  point can be found from the Eq. (11). Velocity difference  $\Delta w_{i-1}$  at the preceding ( $i = 1$ ) point is found using Eq. (15):

$$\Delta w_{i-1} = w_{2(i-1)} - w_{1(i-1)} \quad (15)$$

where  $w_{2(i-1)}$  is hot body velocity at the ( $i = 1$ ) point, m/s;  $w_{1(i-1)}$  is cold body velocity at ( $i = 1$ ) point, m/s.

Fig. 5 shows the energy consumption difference change for the two cases. In the first case hot body moves with the increased velocity, body's energy consumption difference depends on the velocity difference. In the second case cold body moves with the increased velocity. Similarly like in the first case, body's energy consumption difference depends on the speed difference as well. An initial ( $i = 1$ ) point is a starting point for the both cases. The third (middle) curve of the Fig. 5 demonstrates hot body's (lower curve) and cold body's (top curve) energy consumption difference change. It is clear that the increase of the hot body's velocity influences on the energy consumption growth more slowly than in the case of a cold body.

In the Fig. 5 used the following designations:  $Q_i^{hot} - Q_{const}^{hot}$ ;  $Q_i^{cold2} - Q_{const}^{cold2}$  and  $\Delta Q_i - \Delta Q_{const}$  - present the hot body, cold body, and hot and cold bodies' energy consumption difference at the  $i^{th}$  and at the initial ( $i = 1$ ) points;  $w_{2i} - w_{2const}$  - presents the body's velocity differ-

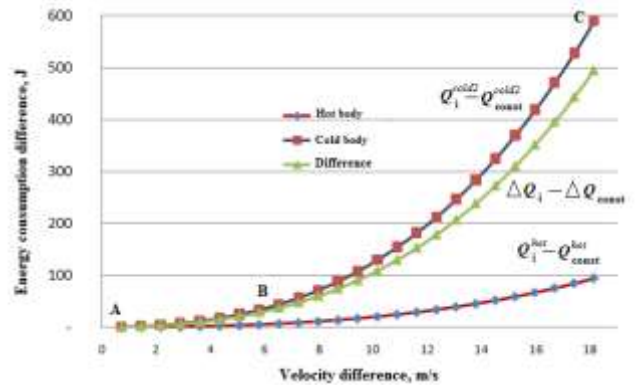


Fig. 5 Hot and cold bodies' energy consumption difference dependence on the velocity difference ( $31000 \leq Re \leq 500000$ ;  $w_{hot} / w_{cold} = 2.5$ )

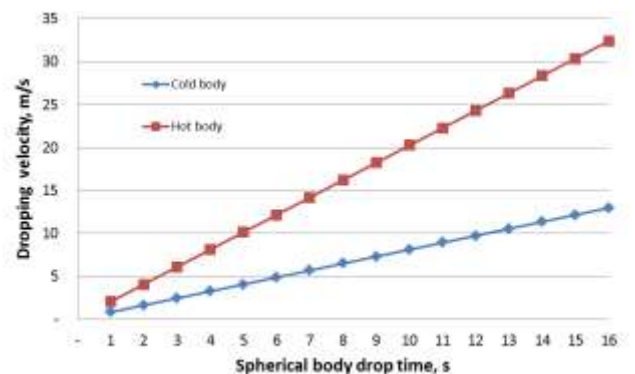


Fig. 6 Hot and cold bodies' velocity dependence on the moving time

ence at the  $i^{th}$  point and at the initial point ( $i = 1$ ). Here the stabilized velocity ( $w_2 = 2.03$  m/s) of the hot body is considered as an initial velocity of the hot and cold bodies.

Fig. 6 shows the hot and cold bodies' velocity changes over the time under the same energy consumption. Hot body velocity grows faster than that of a cold body. On the other hand, it can be stated, that a hot body reaches the same velocity as a cold body using less energy, moreover, during the same time period a hot body goes a longer distance than a cold body.

#### 4. Dynamics of the spherical body drag coefficient changes

As it was already mentioned above, it can be assumed that the drag coefficient of the spherical body is constant ( $C_D = 0.46$ ) for the low velocity  $w \leq 13$  m/s ( $500 \leq Re \leq 200000$ ). Meanwhile, bodies can move at the velocity faster than 13 m/s. In such a case drag coefficient of the spherical body suddenly decreases (Fig. 7). This figure represents an expanded part of the Fig. 1, covering range of  $200000 \leq Re \leq 500000$ .

Using data from the Fig. 7 one can provide the analogous calculation (chapter 3) of the energy consumption for the hot and cold bodies' moving at the velocity greater than 13 m/s. Fig. 8 presents the calculation results. This graph shows that the energy consumption declines if the body's velocity reaches  $\sim 18$  m/s. Energy consumption declination is directly related to the reduction of the drag coefficient  $C_D$  (Fig. 7).

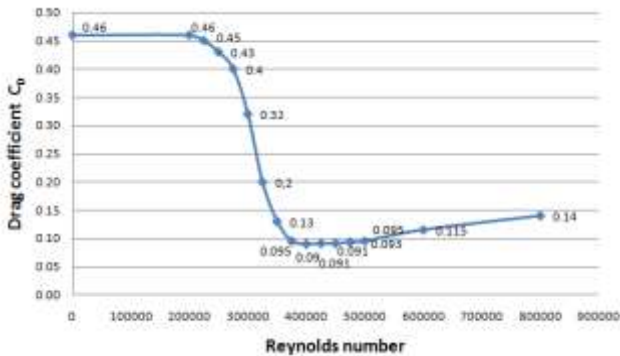


Fig. 7 Body drag coefficient change for the  $200000 \leq Re \leq 500000$  ( $13 \leq w \leq 32$  m/s)

It is possible to stress two turning points (C and D) in the Fig. 8. The first point (C) shows a decrease, and the second one (D) matches an increase of the energy consumption.

Fig. 9 shows a dependence of the relative energy increment on the relative velocity increment. The stabilized velocity ( $w_2 = 2.03$  m/s) is taken as an initial velocity of the hot body.

The relative increment of the energy  $\Delta Q_i / \Delta Q_{const}$  represents a ratio of the energy consumption difference for the cold and hot bodies at the  $i^{th}$  point to the initial energy consumption difference at the initial ( $i = 1$ ) point. Hot body's stabilized velocity ( $w_2 = 2.03$  m/s) is considered as an initial velocity. The relative increment of the velocity  $\Delta w_i / \Delta w_{const}$  represents a ratio of the velocity difference at the  $i^{th}$  point to the initial stabilized velocity ( $w_2 = 2.03$  m/s) difference at the initial ( $i = 1$ ) point.

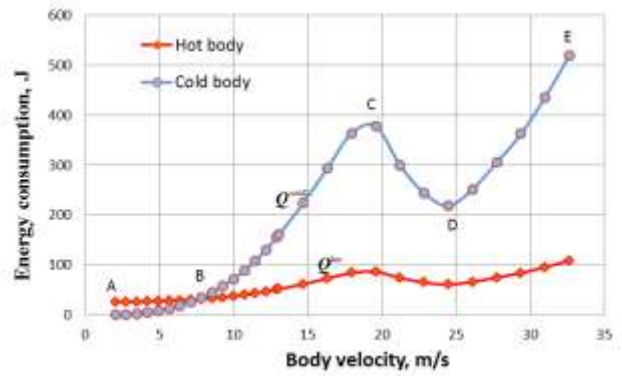


Fig. 8 Hot and cold bodies energy consumption change for the  $31000 \leq Re \leq 500000$  ( $2.03 \leq w \leq 32$  m/s ;  $w_{hot} / w_{cold} = 2.5$ )

The relative increment of the energy  $\Delta Q_i / \Delta Q_{const}$  represents a ratio of the energy consumption difference for the cold and hot bodies at the  $i^{th}$  point to the initial energy consumption difference at the initial ( $i = 1$ ) point. Hot body's stabilized velocity ( $w_2 = 2.03$  m/s) is considered as an initial velocity. The relative increment of the velocity  $\Delta w_i / \Delta w_{const}$  represents a ratio of the velocity difference at the  $i^{th}$  point to the initial stabilized velocity ( $w_2 = 2.03$  m/s) difference at the initial ( $i = 1$ ) point.

A curve part ABC at the Fig. 9 was analyzed previously talking about the curve at the Fig. 5. A curve part CD (Fig. 9), according to the corrected values of the drag coefficient  $C_D$  (Fig. 7), reflects a reduction of the energy consumption. The energy consumption for both hot and cold bodies decreases and the relative increment  $\Delta Q_i / \Delta Q_{const}$  of the energy consumption decreases at the same time also. Further augmentation of the relative velocity influences on the energy consumption increase (curve part DE at the Fig. 9).

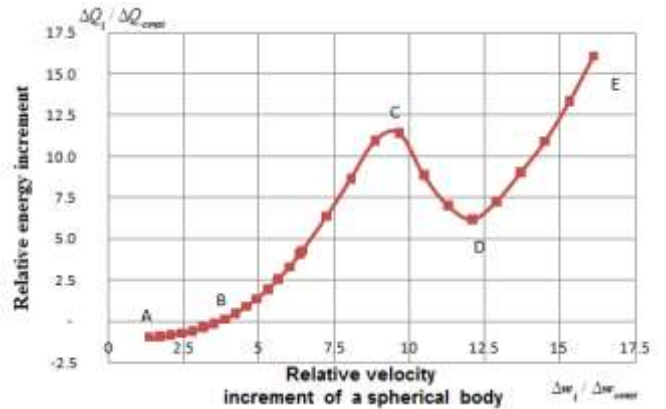


Fig. 9 Energy consumption relative increment for the  $200000 \leq Re \leq 500000$  ( $13 \leq w \leq 32$  m/s ;  $w_{hot} / w_{cold} = 2.5$ )

Fig. 10 reflects a change of the hot and a cold body's energy consumption difference for the curve ABCDE (Fig. 9). The third (middle) curve shows a change of the hot body (lower curve) and cold body (upper curve) energy consumption difference. A starting point, like it was for the previous cases, was considered an initial ( $i = 1$ ) point. A curve part ABC at the Fig. 10 was analyzed more in detail discussing about the curves in the Fig. 5. Similar-

ly, as it was mentioned talking about the Fig. 8 and Fig. 9, the change tendency of the real drag coefficient  $C_D$  (Fig. 7) reflects on the energy consumption decrease (or increase) at the critical points C and D.

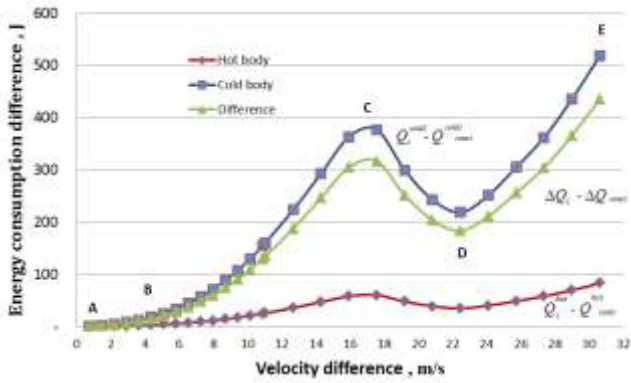


Fig. 10 Energy consumption difference dependence on the velocity difference ( $31000 \leq Re \leq 500000$ ;  $w_{hot}/w_{cold} = 2.5$ )

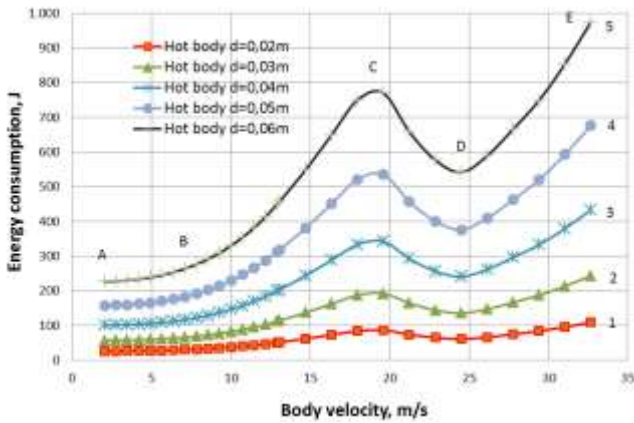


Fig. 11 Hot body diameter influence on the energy consumption change ( $31000 \leq Re \leq 500000$ ;  $w_{hot}/w_{cold} = 2.5$ )

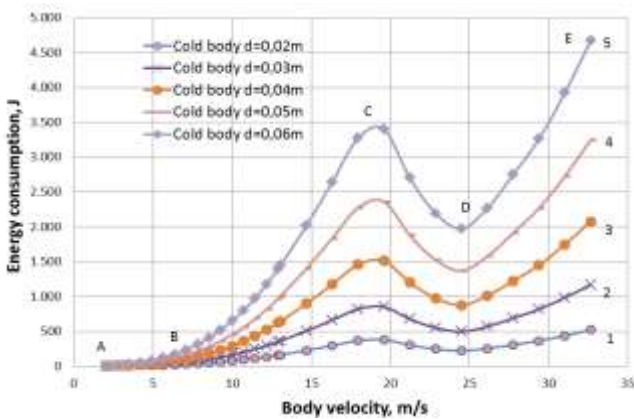


Fig. 12 Cold body diameter influence on the energy consumption change ( $31000 \leq Re \leq 500000$ ;  $w_{hot}/w_{cold} = 2.5$ )

Figs. 11 and 12 show an influence of the hot and cold bodies' diameter on the energy consumption changes. Here also can be noticed the energy consumption decrease (or increase) at the critical points C and D. Those critical points appear at the same vertical line for all the changes of

the body's diameter. This can be explained by the fact that the spherical body's drag coefficient does not depend on the diameter of the body. Meanwhile, spherical body's velocity depends directly on the body size (diameter). Therefore drag force and energy consumption for bigger bodies are higher.

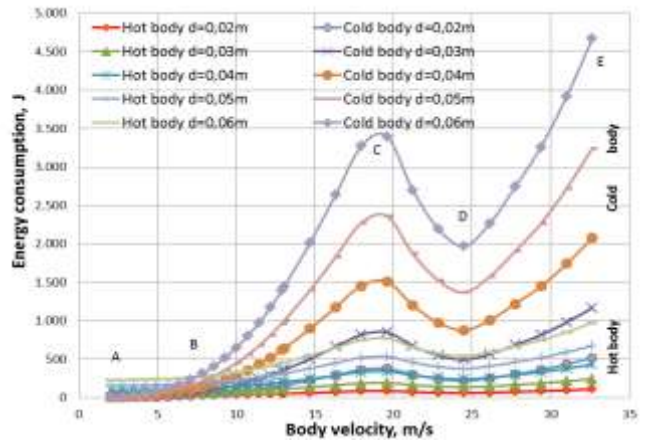


Fig. 13 Hot and cold body's energy consumption comparison ( $31000 \leq Re \leq 500000$ ;  $w_{hot}/w_{cold} = 2.5$ )

The first curve at the Figs. 11 and 12 was analyzed more in detail discussing about the curves in the Fig. 8. It can be noticed that a shape of the curves in the Figs. 11 and 12 are similar each to other, but a magnitude of the energy consumption scale is different. Hot body's energy consumption (Fig. 11) is lower than that of the cold body (Fig. 12). Fig. 13 represents a comparison of the hot and cold body's energy consumption using the same energy scale magnitude.

Figures 11 – 13 show that the bigger body requires more energy consumption. But the hot body moving in the fluid under the boiling crisis conditions (surrounded by the vapour layer) can achieve higher velocity at the lower energy consumption.

### 5. Real case for the body moving in the water

Our experiments [13], which were performed on the hot and cold bodies' moving in water which temperature is less than  $20^\circ\text{C}$ , do not show that the hot body's velocity increases by 2.5 times in comparison with the cold body [7]. Investigation showed that hot body moves in water only 1.2 times faster [11]. For this case hot and cold bodies' energy consumption dependence on the velocity is shown in the Fig. 14. The Fig. 2 and Fig. 8 comparison with the Fig. 14 shows that in this case energy consumption saving starts at higher velocity ( $w = 11.5$  m/s). Furthermore, energy consumption economy Such difference between conditions of the body movement in electrolyte FC-72 and water can be explained by difference in the evaporation heat which is  $i_{fg}^{FC-72} = 88\text{kJ/kg}$  for electrolyte FC-72 and  $i_{fg}^{H_2O} = 2260\text{kJ/kg}$  for water. Otherwise, heat capacity difference influences on the energy consumption as well.

The amount of heat (320.490 MJ), which is required for the  $1\text{ m}^3$  water heating from  $20$  to  $100^\circ\text{C}$ , can be calculated by equation:

$$\dot{Q}_{\text{tot}} = mc_p \Delta T = \rho V c_p (T_3 - T'_3), \quad (16)$$

where  $m$  is water density at the average temperature ( $958.4 \text{ kg/m}^3$  at  $60^\circ\text{C}$ );  $c_p$  is water heat capacity at the same temperature ( $4.18 \text{ kJ/(kg}\cdot\text{K)}$ ).

Using the same Eq. (16) can be found an amount of heat ( $66.530 \text{ MJ}$ ), which is required for the  $1 \text{ m}^3$  electrolyte FC-72 heating from  $20$  to  $56^\circ\text{C}$ . In that case:  $56^\circ\text{C}$  is an electrolyte boiling temperature at the atmospheric pressure;  $m$  is electrolyte density at the average temperature ( $1680 \text{ kg/m}^3$  at  $38^\circ\text{C}$ );  $c_p$  is electrolyte heat capacity at the same temperature ( $1.1 \text{ kJ/(kg}\cdot\text{K)}$ ).

Water heat capacity in comparison with the same of the electrolyte is about 3.8 times higher. At the same time electrolyte boiling (saturation) temperature is about twice less than for water. Therefore the amount of the heat, necessary to reach a boiling point for electrolyte, is about 4.8 times less than for water.

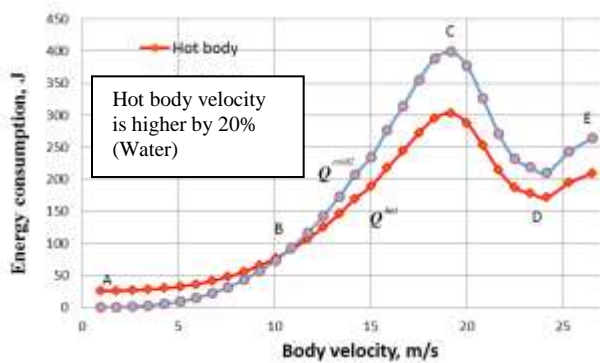


Fig. 14 Hot and cold bodies' energy consumption (Water;  $15000 \leq Re \leq 400000$  ( $0.97 \leq w \leq 26.39 \text{ m/s}$ ;  $w_{\text{hot}}/w_{\text{cold}} = 1.2$ ))

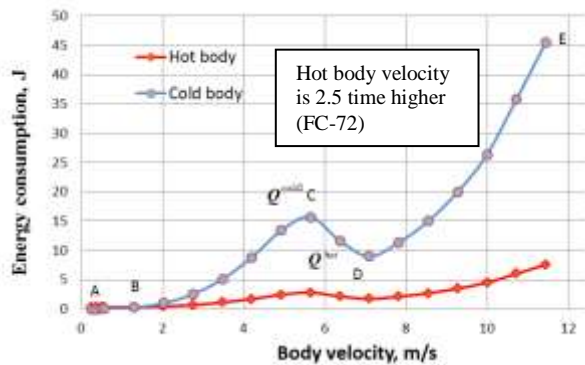


Fig. 15 Hot and cold bodies' energy consumption (Electrolyte FC-72,  $13000 \leq Re \leq 600000$ ;  $0.25 \leq w \leq 11.67 \text{ m/s}$ ;  $w_{\text{hot}}/w_{\text{cold}} = 2.5$ )

Fig. 15 shows the energy consumption for the electrolyte FC-72 when the ratio of the hot body stabilized velocity to the cold body stabilized velocity is 2.5 [7].

According to the Eq. (3), heat flux, necessary to achieve a boiling crisis (Leidenfrost effect) and to form a stable vapour film in the electrolyte is equal to  $0.23 \cdot 10^3 \text{ W/m}^2$ .

It is clear that the energy consumption, necessary to achieve boiling crisis and to form a stable vapour film in the water  $q^{\text{sphere}} = 20 \cdot 10^3 \text{ W/m}^2$  is about 82.6 times higher than that in the case of the electrolyte  $q^{\text{sphere}} = 0.23 \cdot 10^3 \text{ W/m}^2$ . Therefore boiling crisis application

in order to reduce drag force of the moving body, is reasonable in the case of electrolyte, but is doubtful for the water case.

## 6. Conclusions

Hot and cold spherical bodies, moving in the water and electrolyte, energy consumption preliminary comparison shows that:

1. Energy consumption of the hot body, moving in the electrolyte at the velocity, higher than  $1.0 \text{ m/s}$ , is less than that of the cold body.

2. Energy consumption of the hot body, moving in the water at the velocity, higher than  $7.5 \text{ m/s}$  (in the case if the hot and cold bodies' velocity ratio is 2.5), is less than that of the cold body.

3. Energy consumption of the hot body, moving in the water at the velocity, higher than  $11.5 \text{ m/s}$  (in the case if the hot and cold bodies' velocity ratio is 1.2), is less than that of the cold body.

4. Energy consumption of the body, moving in the water, increases with the increase of the velocity up to the  $18 \text{ m/s}$ . Velocity change from  $18 \text{ m/s}$  till  $24 \text{ m/s}$  acts on the energy consumption reduction. Further velocity augmentation influences on the further energy consumption growth.

5. Energy consumption, necessary to achieve boiling crisis on the surface of the spherical body, moving in the water, is about 82.6 times higher than that in the case of the electrolyte.

6. Hot body, surrounded by the vapor film, moves faster, but from the energy economy view, boiling crisis application in order to reduce drag force of the moving body, is reasonable in the case of electrolyte, but is doubtful for the water case.

7. Estimation of the body's velocity influence on the stability of the vapour film, generated on the body's surface, is advisable to include into the further theoretical and experimental investigations.

## References

1. Mills, A.F.; Irwin, R.D. 1995. Basic heat and mass transfer. University of California at Los Angeles, 921p.
2. Yang, J.W.; Park, H.; Chun, H.H.; Ceccio, S.L.; Perlin, M.; Lee, I. 2014. Development and performance at high Reynolds number of a skin-friction reducing marine paint using polymer additives, Ocean Engineering 84: 183–193. <http://dx.doi.org/10.1016/j.oceaneng.2014.04.009>.
3. Makiharju, Simo A.; Perlin, Marc; Ceccio, Steven L. 2012. On the energy economics of air lubrication drag reduction, International Journal of Naval Architecture and Ocean Engineering 4(4): 412–422. <http://dx.doi.org/10.3744/JNAOE.2012.4.4.412>.
4. Vand, A. 1945. Reduction of the skin friction of water by vibration. Patent - US 2366162 A.
5. Babenko, Viktor V.; Chun, Ho-Hwan; Lee, Inwon. 2012. Boundary Layer Flow over Elastic Surfaces: Compliant Surfaces and Combined Methods for Marine Vessel Drag Reduction. Elsevier Science & Technology Books. ISBN: 978-0-12-394806-9.
6. Brennen, C.E. 1995. Cavitation and Bubble Dynamics, Oxford University Press, New York, 236p.
7. Vakarelski, I.U.; Marston, J.O.; Chan, D.Y.C.;

- Thoroddsen, S.T.** 2011. Drag reduction by Leidenfrost vapor layers, *Phys. Rev. Lett.* 106, 214501.  
<http://dx.doi.org/10.1103/PhysRevLett.106.214501>.
8. **Leidenfrost, J.G.** 1966. (C.Wares, Trans., 1966) 1756. *De Aquae Communis Nonnullis Qualitatibus Tractatus.* Duisburg on Rhine, *Int. J. Heat Mass Transfer* 9: 1153–1166.  
[http://dx.doi.org/10.1016/0017-9310\(66\)90111-6](http://dx.doi.org/10.1016/0017-9310(66)90111-6).
9. **Arharov, A.M.; Usaev, S.I.; Kozhinov, I.A.** 1986. *Thermal Engineering, Machine Building.* Moscow. 432p.
10. **Timmerman P.; Jacobus van der Weele, P.** 1998. On the rise and fall of a ball with linear or quadratic drag. *Am. J. Phys.* 67: 538.  
<http://dx.doi.org/10.1119/1.19320>.
11. **Skvorčinskienė, R.; Gyls, J.** 2011. Numerical simulation of the boiling crisis on the sphere surface. *Proceedings of the Thermal power engineering and technologies conference.* February 3–4, Kaunas University of Technology, Kaunas, 158-163.
12. **Zuber, N.** 1959. *Hydrodynamics Aspects of Boiling Heat Transfer.* Atomic Energy Commission Report No. AECU-4439, Physics and Mathematics.
13. **Gyls, J.; Paukštaitis, L.; Skvorčinskienė, R.** 2012. Numerical investigation of the drag force reduction induced by the two-phase flow generating on the solid body surface. *International Journal of Heat and Mass Transfer.* Oxford. Pergamon-Elsevier Science Ltd. 55(25-26): 7645-7650.  
<http://dx.doi.org/10.1016/j.ijheatmasstransfer.2012.07.078>.

J. Gyls, R. Skvorčinskienė, L. Paukštaitis

LEIDENFROSTO EFEKTO YPATUMAI  
PASIPRIEŠINIMO JĖGOS MAŽINIMUI

Re z i u m ė

Straipsnyje pateikiamas šalto (esant aplinkos temperatūrai) ir karšto (apgaubto garų plėvele) sferinio kūno

energijos suvartojimo palyginimas tais atvejais, kai kūnas juda vandenyje ir elektrolite FC-72. Analitinio tyrimo metu laikoma, jog sferinis kūnas yra nerūdijančio plieno, jo skersmuo 0,02 m. Kūno greitis keičiamas nuo 0,03 iki 32,5 m/s; vandens, elektrolito ir šalto kūno temperatūra 20°C; karšto kūno temperatūra 500°C. Analizės metu konstatuota, kad karštas kūnas, apsuptas garų plėvele, juda greičiau. Virimo krizės (Leidenfrosto efekto) taikymas, siekiant sumažinti judančio kūno pasipriešinimo jėgą ir energijos sąnaudas, yra pagrįstas tik tuo atveju, jeigu kūnas juda elektrolite, tačiau abejotinas tuo atveju, kai kūnas juda vandenyje.

J. Gyls, R. Skvorčinskienė, L. Paukštaitis

PECULARITIES OF THE LEIDENFROST EFFECT  
APPLICATION FOR DRAG FORCE REDUCTION

S u m m a r y

An article presents the comparison of the energy consumption of the cold (at an ambient temperature) and hot (wrapped by the vapor film) spherical body, moving in the liquid (water and electrolyte FC-72). Taken in consideration that spherical body is from stainless steel with diameter 0.02 m. Body's velocity was changed from 0.03 to 32.5 m/s; liquid and cold body temperature was kept at 20°C; hot body temperature was equal to 500°C. During the analysis was stated that the hot body, surrounded by the vapor film, moves faster, but from the energy economy view, boiling crisis (Leidenfrost effect) application in order to reduce drag force of the moving body, is reasonable in the case of electrolyte, but is doubtful for the water case.

**Keywords:** drag force, Leidenfrost effect, energy consumption.

Received January 15, 2014

Accepted April 18, 2014